npj | clean water

Article

Published in partnership with King Fahd University of Petroleum & Minerals

https://doi.org/10.1038/s41545-024-00310-z

Energy system for evaluation of modification methods on energy transfer efficiency and optimization of membranes

Tian Li [1,2] ✉, Hong Zhou[1], Wei Ding[1], Jinjun Wang[1] ✉ & Tiancheng Zhang[2] ✉

Saving energy is crucial for utilizing membrane technology, but there is no energy parameter for understanding the relationships among membrane performance and energy. Here, φ is defined as the energy transfer efficiency of the membrane, and its numerical expression of membrane performance is poor (e.g., in the range of 10^{-23}). The method of modifying membranes is a crucial determinant for developing membrane science, but researchers using current parameters to evaluate modification methods might lead to erroneous conclusions. Hence, the newly established system θ is used to analyze the influence of different modification methods on energy consumption, which not only establish the relationship between different modification methods but also provide the research routes for future optimization methods. The main conclusions are as follows: (1) The current modification methods influence on the energy transfer efficiency of the pristine membrane by about $0.4902–3.278 \times 10^4$ times; (2) Using scientific data certifies that the modified support layer of the membranes is a more effective method for reducing the energy consumption than the modified activity layer of the membranes; (3) The establishment of this system provides data support for analyzing the advantages and disadvantages of modification methods, and provides guidance for how to optimize the modification methods of membranes. Therefore, this study not only fills key knowledge gaps in membrane science, but also provides theoretical support for how to optimize membrane modification methods.

Membrane processes are one of the most feasible options for water shortage alleviation and water supply augmentation[1,2]. The essence of membrane science is the process of mass and energy transfer. The key parameters water fluxes J_w, solute fluxes J_s and the mass transfer coefficient k can express the mass transfer effect of membrane[3,4]. However, there is still a lack of energy parameter that can accurately express the energy transfer efficiency. The lack of such key parameters hinders a good understanding of the relationships among membrane operation/performance and energy consumption efficiency.

Researchers have analyzed the relationship between energy conversion efficiency and membrane from various aspects such as electrochemistry, thermodynamics, and external power source[5–9], but there is still no parameter that can express the membrane performance by using the energy transfer efficiency. At present, the FO process is considered a low-energy desalination technology by using the current method to calculate the energy consumption[10–12]. But, current researches confirm that the main reason for the lower water flux is the concentration polarization (CP) in the FO process[13–15]. However, CP of energy consumption should not be neglected under FO mode. The main reason for the result is that the current energy principle uses exogenous energy as the total energy. The existence of knowledge gaps makes it impossible to analyze energy consumption using existing formulas, which leads to the inability to scientifically express the energy transfer efficiency of membrane. Therefore, it is important to establish a novel key parameter to express the energy transfer efficiency of the membrane.

Analyzing the energy transfer efficiency of membrane is aimed at saving energy consumption. There are various efforts to reduce energy consumption such as the optimization of monomer[16,17], introduction of additives[18], thermal post-treatment[19] and use of osmotically driven membrane processes [i.e., forward osmosis (FO) and pressure retarded osmosis (PRO)]. Here, how to evaluate a certain modification method of the membrane is a relatively more effective strategy is very important. At

[1]Southwest University, Chongqing 400715, P. R. China. [2]Civil Engineering Department, University of Nebraska-Lincoln, Omaha, NE, USA.
✉e-mail: lihwang@swu.edu.cn; jjwang7008@yahoo.com; tzhang1@unl.edu

present, the evaluation indicators for membrane modification methods mainly focus on such parameters as water permeability A, volumetric flux of water J_v, and structural parameter S[20–22]. But, the evaluated results might be wrong.

When we introduce a set of data and analyze the current evaluation parameters, it is easy to verify why the conclusion might be incorrect. In one example (Method 1), two different types of highly hydrophilic materials such as silica nanoparticles (SiNPs) and zwitterionic polymers were used to modify polyamide thin-film composite membranes[23]. The value of water permeability, A decreased from 5.778 L/m^2-h-bar to 4.556 L/m^2-h-bar. In another example (Method 2), amine functionalized multi-walled carbon nanotubes was used as an additive in an aqueous solution of 1,3-phenylendiamine to enhance the FO membrane performance[24]. The A value was increased from 3.1 ± 0.04 L/m^2-h-bar to 4.47 ± 0.24 L/m^2-h-bar. These data show that Method 1 has a negative effect on the water permeability, while Method 2 could enhance the water permeability. However, comparing the A values between the two modified can be very confusing or misleading. As far as we know, similar to parameter A, the current membrane parameters are all characterizing parameters that cannot be used to evaluate the improvement in energy consumption and performance of the modified membranes. However, the aforementioned confusing/misleading can be extended to the diverse pristine membranes with different values of the parameters. Hence, there are scientific knowledge gaps: (1) Whether a method has a positive or negative effect on the modification of the membrane performance that cannot be identified by the current parameters; (2) The parameters cannot express how much a modified method can change the membrane performances.

In fact, researchers are more concerned about which the research ideas can be used to achieve the perfect membrane performance. To the best of our knowledge, there is no research that can scientifically guide how to improve membrane performance through data analysis. Researchers need to use an evaluation system to analyze the relative advantages and disadvantages of current modification methods and screen out the research direction with relatively promising development. Finally, researchers need to make a judgment on the research value of self-study modified membrane method through evaluation system. However, when a membrane modification method lacks evaluation system, all modification methods are relatively isolated points. When the research method is independent of other researches, then its scientific significance will be greatly weakened.

In order to fill the key knowledge gaps in the membrane science mentioned above, this article will achieve the following goals: (1) construct a bridge between membrane performance and energy; (2) use an novel evaluation system to evaluate the effect of modification methods on energy transfer efficiency; (3) use data to verify that modifying the support layer is a more effective method than modifying the active layer; and (4) use the evaluation system to provide optimized research routes for future membrane modification methods.

Theoretical framework

The first objective of the study is to establish a new parameter of membrane performance - energy transfer efficiency (φ). The most important concern of membrane science is how much effective energy can remain after a certain amount of initial total energy passes through the membrane. Therefore, we provide the following formula to define this parameter.

$$\varphi = \frac{E_1}{E_0} \tag{1}$$

where, φ as the membrane energy transfer efficiency ($\varphi = E_1/E_0$) to express the energy transformation property of the membrane. E_0 is defined as the initial total energy of the fluid. J. E_1 is defined as the remaining energy of the fluid after passing through the membrane. Therefore, the following derivation will revolve around how to turn E_0 and E_1 into measurable and computable parameters, ultimately leading to the numerical expression of φ. The process of derivation of the following formula follows the principle of simple and easy to obtain.

The total energy of a membrane module can be attributed to the total initial pressure that the solution has before it transports across the membrane. The remaining energy after a certain quantity of water (m_1) passing through the membrane is the effective energy contained by m_1 (e.g., it is available energy for m_1 to move through the chamber downstream of the membrane). The initial total pressure ΔP is the sum of the pressure generated by the salt concentration difference and the external pressure. ΔP as the initial total pressure, there are generally three cases: (1) there is both external pressure and the pressure difference caused by salt concentration, and ΔP is the sum of the two; (2) there is only external pressure and the pressure generated by salt concentration difference is zero. In this case, ΔP is equal to external pressure; (3) there is only the pressure caused by salt concentration difference and the external pressure is zero. In this case, ΔP is equal to the external pressure caused by salt concentration.

When a certain pressure is applied to a fluid, a fluid potential energy is generated. When this pressure is equal to the total initial pressure, the corresponding total initial energy generated by the resulting acting fluid is E_0, J. Assuming that E_0 is the total energy before mass m_0 transport across the membrane, the initial total energy could be assumed to be potential energy or kinetic energy. The purpose of the E_0 formula is to calculate the value of the initial total energy, so the subsequent research is to obtain its value more effectively and simply.

$$E_0 = m_0 g h = \frac{1}{2} m_0 v_0^2 \tag{2}$$

where m_0 is the total mass of water before transporting across the membrane, kg; g is acceleration of gravity, m/s^2; h is an imaginary head that makes m_0 have an initial total energy of E_0, m. Obviously, h corresponds to the total pressure difference (including both mechanical and osmosis pressure) between the two chambers of the membrane; and v_0 is the fluid velocity corresponding to the initial kinetic energy, m/s. When water m_1 passed through the membrane, the total energy contained by m_1 can be determined as:

$$E_1 = \frac{1}{2} m_1 v_1^2 \tag{3}$$

where E_1 is defined as the effective energy contained by m_1, which is essentially the residual energy after m_1 across the membrane, J; m_1 is the quantity of water transporting across the membrane, kg; and v_1 is the permeate water flux (= flow rate) after m_1 crossing the membrane, L/m^2 h. Under different conditions, E_1 will have different formulas to calculate its value. Notice that:

$$m_0 = \rho V_0 = \rho v_0 S t \tag{4}$$

$$m_1 = \rho V_1 = \rho v_1 S t \tag{5}$$

where V_0 is the total volume of water before crossing the membrane, m^3; and V_1 is the water volume after m_1 crossing the membrane, m^3; S is the area of the membrane, m^2; and t is time for m_1 to pass through the membrane, s. Combining Eqs. (3) and (5) leads to the following equation:

$$E_1 = \frac{1}{2} \rho v_1^3 S t \tag{6}$$

Under salt-free condition, term v_1 is $A\Delta P$ with ΔP (There is only external pressure and the pressure generated by salt concentration

difference is zero, ΔP is equal to external pressure). Thus, Eq. 6 becomes:

$$E_1 = E_R = \frac{1}{2}\rho(A\triangle \mathrm{P})^3 St \tag{7}$$

where E_R is the effective energy after pure water m_1 crosses the membrane under the RO mode, J. Under the FO mode or PRO mode (salt condition), J_v is the water permeability of the FO or PRO system, m/s; thus, we have:

$$E_1 = E_F = \frac{1}{2}m_1 J_v^2 = \frac{1}{2}\rho J_v^3 St \tag{8}$$

where E_F is the effective energy after pure water m_1 crossing the membrane under the FO mode or PRO mode, J. Obviously, E_0/St, E_R/St and E_F/St can be considered as energy values per unit area (m^2) and per unit time (s), J/m^2-s.

Notice that for a membrane system $\rho gh = \Delta P$. Thus, from Eq. (1), we have:

$$v_0^2 = \frac{2\triangle \mathrm{P}}{\rho} \tag{9}$$

Combining Eqs. (2, 7, and 9), we have:

$$E_0 = \frac{1}{2}m_0 v_0^2 = m_0\frac{\triangle \mathrm{P}}{\rho} = \rho v_0 St\frac{\triangle \mathrm{P}}{\rho} = \triangle \mathrm{P}\sqrt{\frac{2\triangle \mathrm{P}}{\rho}}St \tag{10}$$

The energy transfer efficiency of the membrane is the more energy that can be transferred through the membrane, the better the membrane performance in terms of the energy transfer efficiency. Therefore, the energy transfer efficiency of membrane is determined by the key parameters: E_0 and E_1. Let's define a parameter, φ as the membrane energy transfer efficiency ($\varphi = E_1/E_0$) to express the energy transformation property of the membrane. By combining Eqs. (5) and (9), φ can be expressed as follows:

$$\varphi = \frac{E_1}{E_0} = \frac{\frac{1}{2}\rho v_1^3 St}{\triangle \mathrm{P}St\sqrt{\frac{2\triangle \mathrm{P}}{\rho}}} = \frac{\rho^{\frac{3}{2}}v_1^3}{2^{\frac{3}{2}}\triangle \mathrm{P}^{\frac{3}{2}}} \tag{11}$$

The parameters involved in this equation are all measurable and calculable; thus, this equation provides sufficient information about the membrane energy transfer efficiency. This parameter φ is the basic parameter of this paper, and parameters such as E_0 and E_1 are used to effectively obtain the value of parameter φ. Therefore, the derivation direction of these formulas is practical, measurable and computable. Now, let's analyze the numerical change of parameter φ under the RO, FO, or PRO mode. Under the RO mode ($v_1 = A$), Eq. (11) becomes:

$$\varphi = \varphi_R = \frac{v_1^3\rho^{\frac{3}{2}}}{2^{\frac{3}{2}}\triangle \mathrm{P}^{\frac{3}{2}}} = \frac{\rho^{\frac{3}{2}}A^3}{2^{\frac{3}{2}}\triangle \mathrm{P}^{\frac{3}{2}}} \tag{12}$$

where φ_R is the membrane energy transfer efficiency under the RO mode. Under the FO ($v_1 = J_v$) or PRO mode ($v_1 = J_v$), we have:

$$\varphi = \varphi_F = \varphi_P = \frac{\frac{1}{2}m_1 v_1^2}{\frac{1}{2}m_0 v_0^2} = \frac{\rho^{\frac{3}{2}}J_v^3}{2^{\frac{3}{2}}\triangle \mathrm{P}^{\frac{3}{2}}} \tag{13}$$

When the initial reference points of the two membrane processes are different, it is difficult (or even impossible) to use the existing parameters in the current literatures to evaluate which method improves the membrane performance more effectively. The initial benchmark values must be consistent (or at least transformable) when comparing the effects of different methods on the performance of the modified membranes. Therefore, in this study, we propose a new parameter θ –the energy transfer efficiency ratio– to compare the effective energy of the modified membrane with that of the pristine membrane as follows:

$$\theta = \frac{E_{1m}}{E_{1p}} = \frac{\frac{1}{2}m_{1m}v_{1m}^2}{\frac{1}{2}m_{1P}v_{1P}^2} = \frac{\rho v_{1m}St}{\rho v_{1P}St}\times\left(\frac{v_{1m}}{v_{1P}}\right)^2 = \left(\frac{v_{1m}}{v_{1P}}\right)^3 or\theta = \frac{E_{1m}}{E_{1P}} = \frac{\frac{E_{1m}}{E_0}}{\frac{E_{1P}}{E_0}} = \frac{\varphi_{1m}}{\varphi_{1P}} \tag{14}$$

where E_{1m} and E_{1P} are the effective energy of the modified and pristine membrane, respectively, J ; v_{1m} and v_{1p} are the permeate water flux after crossing the modified and pristine membrane, respectively, m/s; φ_{1m} and φ_{1P} are the membrane energy coefficient of the modified and pristine membrane, respectively, unitless. Under the same initial process conditions, the value of the modified membrane parameter v_{1p} and the value of the pristine membrane parameter $v_{1\mathrm{m}}$ could be measured. Here, as long as we can measure the values of these two parameters, then we can obtain the value of the evaluation system θ. The definable conditions of parameters $v_{1\mathrm{m}}$ and $v_{1\mathrm{p}}$ determine the applicable range of parameter θ. However, the measurement of the two parameters is not conditionally limited. Hence, this novel evaluation system θ could be applicable to any type of water treatment membrane (MF, UF, RO etc).

Under the RO mode, we have:

$$\theta = \theta_R = \frac{E_{1m}}{E_{1P}} = \left(\frac{A_m}{A_P}\right)^3 \tag{15}$$

where θ_R is the energy transfer efficiency ratio under the RO mode; and A_m and A_P are the water permeability of the modified and pristine membrane, respectively, m^3/m^2-s-bar. Under FO or PRO mode, we have:

$$\theta = \theta_F = \theta_P = \frac{E_{1m}}{E_{1P}} = \left(\frac{J_{vm}}{J_{vP}}\right)^3 \tag{16}$$

where θ_F and θ_P are the energy transfer efficiency ratios of the FO and PRO mode, respectively; and J_{vm} and J_{vP} are the water permeability of the modified and pristine membrane, respectively, m/s. The derivation process of the above formula accords with the basic fluid dynamics equations[25].

Results and discussion

Energy transfer efficiency of membranes with different structures and operational modes

From Table 1, the similarity and difference between energy expression parameter φ and current parameters A and J_v for different conventional membranes and modes are analyzed. Parameters A and J_v are similar to the energy parameter φ to express the membrane performances. The larger the values of A, J_v and φ are, the better the membrane performance is. As shown in Columns 3 A and 6 A, Parameters A and φ represent the same sequence of membrane performance from good to bad: Asymmetric TFC hollow fiber > Positively charged hollow fiber > doubled-skinned flat-sheet membrane > TFC hollow fiber > TFC flat-sheet membrane and commercial asymmetric flat-sheet membrane > Symmetric flat-sheet membrane. The parameter φ shows the same trend of change as A and J_v do. For instance, under FO or PRO mode, the commercial asymmetric flat-sheet membrane (J_v = 18.30 L/m^2 h, $\varphi_F = 4.368\times10^{-23}$ or $\varphi_P = 3.408\times10^{-22}$) has a better membrane performance than the TFC flat-sheet membrane (J_v = 15.79 L/m^2 h, $\varphi_F = 2.905\times10^{-23}$ or $\varphi_P = 1.967\times10^{-22}$), while the φ_R and A values of the two membranes were the same under the RO mode (Table 1). Hence, the membrane performance can be expressed by the energy transfer efficiency, but under different process conditions, the values of the energy transfer efficiency will be different.

However, parameter φ has its own unique function. Parameter φ, as an energy expression parameter, can reflect the relationship between different membranes and energy. In the absence of salt, the φ_R values of conventional membranes range from 9.892×10^{-27} to 2.245×10^{-21}. Under the FO or PRO mode, the range for parameter $\varphi_{F/P}$ is still very low (2.540×10^{-24} ~ 5.020×10^{-22}). These results demonstrate that the energy consumption of

Table 1 | Membrane energy transfer efficiency coefficients affected by different membrane structures and operational modes

1 A Membrane Structure	2 A Material	3 A Pure water permeability A (L/m^2 h bar)	4 A Initial total energy E_0 (J/ m^{2}S bar)/St	5 A Permeability energy E_{1R} (J/ m^2 S bar)/St	6 A Energy transfer efficiency φ_R	7 A Ref
TFC flat-sheet membrane	Polyamide–polysulfone	1.19	1.442×10^6	1.806×10^{-17}	1.252×10^{-23}	61
Commercial asymmetric flat-sheet membrane	Cellulose tricetate	1.19 ± 0.19	1.442×10^6	1.806×10^{-17}	1.252×10^{-23}	62
Symmetric flat-sheet membrane	Carboxylated poly (aryl ether sulfone) (PAES-COOH)	0.11	1.442×10^6	1.426×10^{-20}	9.892×10^{-27}	63
Double-skinned flat-sheet membrane	double-polyamide	1.983 ± 0.01	1.442×10^6	2.300×10^{-17}	1.595×10^{-23}	64
TFC hollow fiber	Polyamide–polyethersulfone	1.68	1.442×10^6	5.083×10^{-17}	3.524×10^{-23}	65
Asymmetric TFC hollow fiber	Polyvinyl chloride	6.71	1.442×10^6	3.238×10^{-15}	2.245×10^{-21}	66
Positively charged hollow fiber	Poly(amideimide)-polyethyleneimine	6.25	1.442×10^6	2.616×10^{-15}	1.814×10^{-21}	67
1B	2B	3B	4B	5B	6B	7B
Membrane	Feed solution /Draw solution	Pure water flux J_v under FO mode (L/m^2-h)	E_0 (J/ m^{2}S)/st	Energy transfer efficiency φ_F	Pure water flux J_v under PRO mode (L/m^2 h)	Energy transfer efficiency φ_P
TFC flat-sheet membrane	10 mM NaCl/2 M NaCl	15.79	1.455×10^9	2.905×10^{-23}	29.89	1.967×10^{-22}
Commercial asymmetric flat-sheet membrane	10 mM NaCl /2 M NaCl	18.30	1.455×10^9	4.368×10^{-23}	35.90	3.408×10^{-22}
Symmetric flat-sheet membrane	DI water /2 M NaCl	7.03	1.466×10^9	2.540×10^{-24}	~	~
Double-skinned flat-sheet membrane	DI water/2 M NaCl	16.19	1.466×10^9	3.102×10^{-23}	40.95	5.020×10^{-22}
TFC hollow fiber	DI water/1 M NaCl	25.11	5.183×10^8	3.174×10^{-22}	~	~
Asymmetric TFC hollow fiber	DI water/2 M NaCl	35	1.466×10^9	3.158×10^{-22}	40	4.713×10^{-22}
Positively charged hollow fiber	DI water/1.5 M $MgCl_2$	12.94	3.306×10^9	7.023×10^{-24}	17.82	1.834×10^{-23}

Columns A in RO mode; columns 3B and 5B in FO mode; columns 6B and 7B in PRO mode. The initial total pressure of fluid in columns A is 1bar, and the initial total pressure (ΔP) of fluid in columns B are produced by the salt concentration differences. Column 4A is calculated based Eq. (9) (e.g., $1.442 \times 10^6 = \frac{st}{st} \times 1.013 \times 10^5 \times \sqrt{\frac{1.013 \times 10^5 \times 2}{1000}}$). Column 5A is calculated based on Column 3A and Eq. (6) [e.g., $1.806 \times 10^{-17} = 1/2 \times 10^3 \times (\frac{1.19}{3600 \times 1000})^3$]. Column 6A is calculated based on Column 4A and 5A and Eq. (10) [e.g., $1.252 \times 10^{-23} = (1.806 \times 10^{-17}) / (1.442 \times 10^6)$]. Column 4B is calculated based on 2B and Eq. (9) [e.g. $1.455 \times 10^{-9} = 100.5945 \times 1.013 \times 10^5 \times \sqrt{2 \times 1.013 \times 10^5 \times 100.5945/1000}$] ($P_A$-$P_B$ is calculated based on empirical van't Hoff equation). Column 5B is calculated based on Column 3B and Column 4B Eq. (12) [e.g. $2.905 \times 10^{-23} = (1/2 \times 10^3) \times [15.79 / (3600 \times 1000)]^3 / 1.455 \times 10^9$]. Column 7B is calculated based on Column 6B and Column 4B Eq. (12). {e.g. $1.967 \times 10^{-22} = (1/2 \times 10^3) \times [29.89/(3600 \times 1000)]^3 \times \frac{St}{St} / 1.455 \times 10^9$]}.

the membrane is huge. Thus, it is very important to find ways to improve the energy transfer efficiency and to establish an evaluation system for the methods of modifying the membrane.

In this study, the energy transfer efficiency is calculated by analyzing two key parameters instead of building a conventional model. First, let's analyze the knowledge bottleneck existing in conventional research. This kind of research mainly through the establishment of theoretical model, analysis of the energy consumption of the membrane, calculation of energy transfer efficiency. The core problem in establishing this theoretical model is that the membrane structure is complicated, which makes it impossible to describe the specific fluid mass transfer route. The main idea to solve this research is to simplify the model through theoretical assumptions and use exogenous energy consumption as the energy consumption of the membrane. The theory assumes a simplified model, which causes the theoretical model to be far away from the internal structure of the actual membrane, such as the two typical theories of mass transfer theory—the solution-diffusion model and the pore flow model[26–29]. One theory assumes that the membrane has no pores and is homogeneous, while the other assumes that the pores in the membrane are square. Hence, the energy consumption using such models is not only due to the large difference between the internal resistance structure of the membrane and the actual situation, but also because different models will have different results, so the final energy transfer efficiency of the membrane is not of universal practical significance. When researchers use exogenous energy consumption to analyze energy consumption, they ignore the salt concentration difference with large energy (Table 1). Due to the complex structure of membrane, the energy theory of membrane is still a black-box nature. Therefore, there are still some key knowledge gaps in the analysis of fluid energy transfer efficiency by conventional methods.

However, the present study uses two key parameters E_0 and E_1 to calculate the energy transfer efficiency value, which effectively avoids the above drawbacks. The values of the two parameters are independent of the energy transfer process. Therefore, the energy transfer efficiency calculated by this method is independent of how and in what form the energy is transferred. Because only the residual energy of the fluid after passing the membrane is the effective energy, the fluid energy that the fluid bounces back from the membrane and the energy that remains in the membrane are invalid energy. When the initial total energy is determined, the remaining energy of fluid is the larger, and the energy transfer efficiency of the membrane is the higher. The method developed in this study for calculating energy transfer efficiency is not only simple and practical, but also universal because the values of this parameter can be calculated via measurable data, making the method be objectivity and reliable.

Using energy parameters to evaluate the effects of modifying membranes' active layers

There is rapid growth in studying FO membranes[30–32] and FO-based applications[33–41]. The FO membrane includes two layers-an active layer and a support layer. Significant efforts have been made to improve the active layer by focusing on: surface hydrophobicity[42,43], membranes pore structure[44], internal concentrative concentration polarization[45], surface roughness[46] and pore size distribution[47]. So far, the modified membranes are evaluated on the basis of water/salt permeability coefficients; limited information is available on how the modifications would affect energy transfer efficiency of the membranes. Herein, we found that modifying the characteristics of the active layer with different strategies (four shown in Table 2) may affect the energy parameters (φ and θ) under the RO, FO, and PRO mode. Below, parameters φ and θ use the data to show the influence of the modified activated layer on the energy transfer efficiency.

There are two kinds of modification methods for expression parameters evaluation: (1) Evaluation of different methods for modifying the properties of the same membrane; (2) Evaluation of the different methods for modifying the properties of the different membranes. In the first case, using the current parameter evaluation will not produce wrong conclusions, which are consistent with the evaluation results of the evaluation system. Fixed the pristine membrane, the values of all parameters (A, J_v, φ and θ) are in the same order from small to large. (Table 2). For example, when the initial membrane is TFC^2 (control), the A value rises from 3.1 ± 0.04 L/m^2 h bar to 4.47 ± 0.24 L/m^2 h bar, the corresponding θ_R increases from 2.214×10^{-22} to 6.620×10^{-22}, and when J_v increases from 11.43 L/m^2 h to 32.8 L/m^2 h, the corresponding θ_F rises from 1 to 23.76, and the corresponding θ_P rises from 1 to 12.84.

In the second case, the results of modification methods evaluated by expression parameters (A, J_v and φ) apparent parameters and evaluation parameter (θ) are quite different. Under RO mode, the φ_R and A values of the modified membranes have the following order: TFC^4—3 > TFC^1-1 and TFC^1-2 > TFN ^{2}-3 > TFC^3-3 > TFN5-3, and the θ of the modified membranes have the other following order: TFC^3-3 (39.68) > TFN^5-3 (11.80) > TFC^4-3 (4.184) > TFN ^{2}-3 (2.990) > TFC^1-1 (0.4902) and TFC^1-2 (0.4902); Under FO mode, the φ_R values of the modified performance of membranes from the best to the worst were as follows: TFC^3-3 > TFN^2-3 > TFN^5-3 > TFC^4-3, and the θ values of the modified membranes from large to small were as follows: TFC^3-3 (23.76) > TFN^5-3 (6.785) > TFC^4-3 (3.980) > TFN^2-3(2.974); Under PRO mode, the φ_P values from high to low were as follows: TFN^2-3 > TFC^3-3 > TFC^4-3 > TFN^5-3, and the θ values of the modified membranes from high to low were as follows: TFN ^{2}-3 (17.84) > TFC^3-3 (12.84) > TFC^4-3 (5.136) > TFN^5-3 (3.279). What are the reasons for this? Is it related to the inability of expression parameters to evaluate the modification method?

The following takes the evaluation result of parameter A as an example: in Method 1, two additional different types of highly hydrophilic materials (i.e., silica nanoparticles (SiNPs) and zwitterionic polymers) can modify polyamide thin-film composite membranes[23]. The A value was decreased 5.778 L/m^2 h bar to 4.556 L/m^2 h bar; in Method 2, amine functionalized multi-walled carbon nanotubes were used as additive in aqueous solution of 1,3-phenylendiamine to enhance the FO membranes performance[48]. The A value increased from 1.12 L/m^2 h bar to 3.82 L/m^2 h bar. These data show that method 1 has a negative impact on the parameter A, while method 2 has a positive impact on the parameter A. However, up comparing the value of parameter A of method 1 and the value of parameter A of method 2 of the modified membrane, it is interesting note the wrong conclusion regarding utilization of parameter A. Hence, the result demonstrates that the current parameters are unable to evaluate membrane modification methods.

It is well-known that the performances of the different pristine membranes are different (i.e., inconsistent). Thus, only after removing the influences of the different pristine membranes can eliminate the error. Therefore, the evaluation system takes the energy transfer efficiency of different pristine membranes as the denominator, and the energy transfer efficiency of different modified membranes as the numerator, and calculates the values. Using the energy transfer efficiency ratio of the pristine membrane θ as a benchmark, the criteria can be established as follows: (1) for the modification of a single membrane: if $\theta = 1$, no improvement; if $\theta < 1$, a negative improvement; and if $\theta > 1$, a positive improvement effect on the energy transfer efficiency of the membrane; (2) for comparison between different modification methods: a larger θ value indicates more improvement. Therefore, parameter θ can be used as an evaluation system to analyze the influence of different methods on the energy transfer efficiency.

The maximum energy transfer efficiency of the modified activation layer can reach 39.68 times of that of the pristine membrane, while the minimum energy transfer efficiency of the modified activation layer is only 0.4902 times. These results show that modified activation layer is an effective way to reduce energy consumption, but there is still a lot of room for improvement.

Using energy parameters to evaluate the effects of modifying membranes' supporting layers

Various studies have been explored to optimize the support layers by incorporating hydrophilic polymer[49], inorganic nano-particles[50,51], pore forming agents[52,53] into the membrane substrate, or by altering the coagulation bath during the membrane formation[54], and so on. However, these two knowledge gaps remain in the research as follows: (1) how much influence do the modified support layers have on the energy consumption of the membranes; (2) what is the energy transfer efficiency of the support layers modified by different strategies?

Analyzing the impact on the energy transfer efficiency of the same pristine membrane, the trends of the characterization parameter (e.g., A, J_v and φ) and evaluation parameter (θ) are consistent (Tables 2, 3). The differences between Tables 3, 2 are analyzed below.

Table 3 shows that the energy transfer efficiency is effectively improved by modifying the supporting layer in the RO mode, FO mode, and PRO mode. By comparing the data in Tables 2, 3, it is shown digitally for the first time that the modified support layer has greater potential to improve the energy transfer efficiency of the membrane than the modified active layer. The maximum θ values of the influence of the modified activation layer on the energy transfer efficiency in the RO mode, FO mode, and PRO mode are 39.68, 23.76 and 17.84, respectively (Table 2). The maximum θ values of the modified support layer are 1.969×10^4, 3.278×10^4, and 1.652×10^4 in the RO mode, FO mode, and PRO mode, respectively. The results further prove that the support layer has more influence on the fluid transfer than the active layer[54]. Therefore, these results indicate that the modified support layer has greater potential to improve the energy transfer efficiency of the membrane than the modified activation layer.

Using energy parameters to evaluate the effects of modifying membranes' single factor or structure

For a long time, it has been recognized that modifying the structure of the membranes would mitigate internal concentration polarization (ICP). However, up to now, it is often difficult to evaluate the relative effectiveness of these methods because different strategies were used to modify these membranes due to different structure and chemical properties of the pristine membranes. For example, the value of the structural parameter S is a direct indicator of the ICP[55–57], which can be determined by using the classical ICP model developed before[58]. However, simply comparing the S_c values among different methods (Table 4), it would be difficult for one to determine the effectiveness of different modification methods on the membrane properties. As shown in Table 4 and Fig. 1, the relationships among S_c and the energy transfer efficiency of modified membranes can be evaluated, for the first time, via the two energy parameters. Taking the modified membrane parameter S as the numerator and the pristine membrane parameter S_c as the denominator, the change rate of the ratio S/S_c and the regression equations are as follows: (1) hydroxyl functionalized

Table 2 | Energy parameters affected modifying the active layer of the membranes and operational modes

1 A Membrane	2 A Active layer	3 A Pure water permeability A (L/m^2-h bar)	4 A E_0/st (J/ m^2-S bar)	5 A E_g/st (J/m^2-S bar)	6 A Energy conversion efficiency φ_R	7 A Energy conversion efficiency ratio θ_R	8 A Ref
TFC$^{1\,(control)}$	TFC	5.778	1.442×10^{6}	2.067×10^{-15}	1.433×10^{-21}	1	23
TFC^{1}−1	SiNP-TFC	4.556	1.442×10^{6}	1.013×10^{-15}	7.025×10^{-22}	0.4902	23
TFC^{1}-2	PSBMA-TFC	4.556	1.442×10^{6}	1.013×10^{-15}	7.025×10^{-22}	0.4902	23
TFC$^{2\,(control)}$	Control	3.1 ± 0.04	1.442×10^{6}	3.193×10^{-16}	2.214×10^{-22}	1	24
TFN^{2}-1	F-MWCNTs (0.01 w/v%)	3.44 ± 0.2	1.442×10^{6}	4.363×10^{-16}	3.025×10^{-22}	1.366	24
TFN^{2}-2	F-MWCNTs (0.05 w/v%)	3.6 ± 0.16	1.442×10^{6}	5.000×10^{-16}	3.467×10^{-22}	1.566	24
TFN^{2}-3	F-MWCNTs (0. 1 w/v%)	4.47 ± 0.24	1.442×10^{6}	9.572×10^{-16}	6.620×10^{-22}	2.990	24
TFC$^{3\,(Control)}$	Control	1.12	1.442×10^{6}	1.506×10^{-17}	1.044×10^{-23}	1	48
TFC^{3}-1	NH_2-TNTs (0.01 w/v%)	1.69	1.442×10^{6}	5.173×10^{-17}	3.587×10^{-23}	3.435	48
TFC^{3}-2	NH_2-TNTs (0.05 w/v%)	2.39	1.442×10^{6}	1.463×10^{-16}	1.015×10^{-22}	9.713	48
TFC^{3}-3	NH_2-TNTs (0.1 w/v%)	3.82	1.442×10^{6}	5.974×10^{-16}	4.143×10^{-22}	39.68	48
TFC$^{4\,(control)}$	Control	3.09 ± 0.06	1.442×10^{6}	3.162×10^{-16}	2.193×10^{-22}	1	68
TFC^{4}-1	Zwitterion TFC-10	3.34 ± 0.04	1.442×10^{6}	3.993×10^{-16}	2.769×10^{-22}	1.263	68
TFC^{4}-2	Zwitterion TFC-30	4.81 ± 0.03	1.442×10^{6}	1.193×10^{-15}	8.273×10^{-22}	3.772	68
TFC^{4}-3	Zwitterion TFC-50	4.98 ± 0.05	1.442×10^{6}	1.323×10^{-15}	9.175×10^{-22}	4.184	68
TFC$^{5(control)}$	Control	1.12	1.442×10^{6}	1.506×10^{-17}	1.044×10^{-23}	1	69
TFN^{5}-1	HNTS (0.01 w/v%)	1.53	1.442×10^{6}	3.838×10^{-17}	2.662×10^{-23}	2.550	69
TFN^{5}-2	HNTS (0.05 w/v%)	1.86	1.442×10^{6}	6.896×10^{-17}	4.782×10^{-23}	4.580	69
TFN^{5}-3	HNTS (0.1 w/v%)	2.55	1.442×10^{6}	1.777×10^{-16}	1.232×10^{-22}	11.80	69
1B Membrane	**2B Feed solution/draw solution**	**3B Pure water flux J_v (L/m^2-h)**	**4B $\varphi_F = \frac{E_{1F}}{E_0}$ under FO mode**	**5B θ_F under FO mode**	**6B J_v Pure water flux (L/m^2-h bar) under PRO mode**	**7B $\varphi_P = \frac{E_{1F}}{E_0}$ under PRO mode**	**8B θ_P under PRO mode**
TFC$^{2\,(control)}$	10 mM NaCl/ 2 M NaCl	27.06	1.459×10^{-22}	1	36.47	3.573×10^{-22}	1
TFN^{2}-1	10 mM NaCl/ 2 M NaCl	28.24	1.659×10^{-22}	1.137	67.06	2.221×10^{-21}	6.216
TFN^{2}-2	10 mM NaCl/ 2 M NaCl	30.59	2.108×10^{-22}	1.445	74.12	2.999×10^{-21}	8.394
TFN ^{2}-3	10 mM NaCl/ 2 M NaCl	38.82	4.339×10^{-22}	2.974	95.29	6.373×10^{-21}	17.84
TFC$^{3\,(Control)}$	10 mM NaCl/ 1 M NaCl	11.43	3.155×10^{-23}	1	21.05	1.958×10^{-22}	1
TFC^{3}-1	10 mM NaCl/ 1 M NaCl	14.93	6.986×10^{-23}	2.229	24.29	3.008×10^{-22}	1.536
TFC^{3}-2	10 mM NaCl/ 1 M NaCl	21.43	2.066×10^{-22}	6.590	31.43	6.518×10^{-22}	3.329
TFC^{3}-3	10 mM NaCl/ 1 M NaCl	32.86	7.449×10^{-22}	23.76	49.29	2.530×10^{-21}	12.84
TFC$^{4\,(control)}$	DI water/1 M NaCl	10.11	2.137×10^{-23}	1	20.09	1.677×10^{-22}	1
TFC^{4}-1	DI water/1 M NaCl	10.91	2.685×10^{-23}	1.256	21.82	2.148×10^{-22}	1.281
TFC^{4}-2	DI water/1 M NaCl	15.91	8.327×10^{-23}	3.897	27.73	4.409×10^{-22}	2.629
TFC^{4}-3	DI water/1 M NaCl	16.45	8.505×10^{-23}	3.980	29.85	5.499×10^{-22}	3.279
TFC$^{5(control)}$	10 mM NaCl/ 2 M NaCl	13.33	1.745×10^{-23}	1	24.29	1.055×10^{-22}	1
TFN^{5}-1	10 mM NaCl/ 2 M NaCl	17.62	4.029×10^{-23}	2.309	30.05	1.999×10^{-22}	1.895
TFN^{5}-2	10 mM NaCl/ 2 M NaCl	20.86	6.686×10^{-23}	3.832	34.29	2.969×10^{-22}	2.814
TFN^{5}-3	10 mM NaCl/ 2 M NaCl	25.24	1.184×10^{-22}	6.785	41.90	5.418×10^{-22}	5.136

Note: columns A under RO mode, columns B under FO mode and PRO mode. Calculation methods for Columns 1-6A, Columns 4B and 6B are similar to other used in Table 1. The initial total pressure of fluid in columns A is 1bar, and the initial total pressure (ΔP) of fluid in columns B are produced by the salt concentration differences. Column 7A is calculated based on Column 5A Eq. (14) [e.g., 0.4902 = (4.556 / (5.778)3]). Column 5B is calculated based on column 3B and Eq. (15) [e.g., 1.137 = (28.24 / 27.06)3]. Column 7B is calculated based on column 3B and Eq. (15) [e.g., 6.216 = (67.06 / 36.47)3].

Table 3 | Energy parameters affected modifying the support layer of the membranes and operational modes

1 A Membrane	2 A Support layer	3 A Pure water permeability A (L/m^2-h bar^{-1})	4 A Initial total energy E_0/st (J/m^2-S bar)	5 A Effective energy E_1/st $(\frac{1}{2}mv_1^2)$ (J/ m^2-S bar)	6 A Energy transform efficiency $\varphi_R = \frac{E_{1R}}{E_0}$	7 A Effective energy ratio coefficient $\theta_R = \frac{E_{1m}}{E_{1P}}$	8 A Ref
TFC[1] control	(21/0/79) wt%, PVDF/PFSA/NMP	0.11 ± 0.01	1.442×10^6	1.426×10^{-20}	9.889×10^{-27}	1	70
TFC[1] MT-1	(20/1/79) wt%, PVDF/PFSA/NMP	0.57 ± 0.12	1.442×10^6	1.985×10^{-18}	1.377×10^{-24}	139.2	70
TFC[1] MT-2	(19/2/79) wt%, PVDF/PFSA/NMP	1.49 ± 0.09	1.442×10^6	3.545×10^{-17}	2.458×10^{-23}	2486	70
TFC[1] MT-3	(18/3/79) wt%, PVDF/PFSA/NMP	2.97 ± 0.06	1.442×10^6	2.808×10^{-16}	1.947×10^{-22}	1.969×10^4	70
TFC[1] MT-5	(16/5/79) wt%, PVDF/PFSA/NMPe	2.31 ± 0.16	1.442×10^6	1.321×10^{-16}	9.161×10^{-23}	9264	70
TFC[2] Control	(18/3/0) wt%, PVDF/PVP/SiO_2@MWNTs	0.83 ± 0.03	1.442×10^6	6.131×10^{-18}	4.252×10^{-24}	1	71
TFC[2] MS-10	(18/3/0.1) wt%, PVDF/PVP/SiO_2@MWNTs	0.89 ± 0.01	1.442×10^6	7.553×10^{-18}	5.237×10^{-24}	1.232	71
TFC[2] MS-25	(18/3/0.25) wt%, PVDF/PVP/SiO_2@MWNTs,	1.04 ± 0.06	1.442×10^6	1.206×10^{-17}	8.363×10^{-24}	1.967	71
TFC[2] MS-50	(18/3/0.5) wt%, PVDF/PVP/SiO_2@MWNTs	1.16 ± 0.02	1.442×10^6	1.672×10^{-17}	1.160×10^{-23}	2.728	71
TFC[2] MS-75	(18/3/0.75) wt%, PVDF/PVP/SiO_2@MWNTs	1.21 ± 0.01	1.442×10^6	1.898×10^{-17}	1.316×10^{-23}	3.095	71
TFC[2] MS-100	(18/3/1) wt%, PVDF/PVP/SiO_2@MWNTs	1.02 ± 0.02	1.442×10^6	1.137×10^{-17}	7.885×10^{-24}	1.854	71
TFC[3] Control	(17.50/82.00/0.00) wt%, PSf /NMP/TiO_2	1.19	1.442×10^6	1.807×10^{-17}	1.253×10^{-23}	1	61
TFC[3] TFN0.5	(17.41/81.59/0.50) wt%, PSf /NMP/TiO_2	1.96	1.442×10^6	8.067×10^{-17}	5.594×10^{-23}	4.464	61
TFC[3] TFN0.75	(17.36/81.39/0.75) wt%, PSf/NMP/TiO_2	2.85	1.442×10^6	2.481×10^{-16}	1.721×10^{-22}	13.74	61
TFC[3] TFN1	(17.33/81.18/0.99) wt%, PSf/NMP/TiO_2	2.98	1.442×10^6	2.836×10^{-16}	1.967×10^{-22}	15.70	61

1B Membrane	2B Feed solution/ Draw solution	3B Pure water flux J_v under FO mode (L/m^2-h)	4B $\varphi_F = \frac{E_{1F}}{E_0}$ under FO mode	5B θ_F under FO mode	6B Pure water flux J_v under PRO mode (L/m^2-h)	6B $\varphi_P = \frac{E_{1F}}{E_0}$ under PRO mode	7B θ_F under PRO mode
TFC[1] Control	DI water/1 M NaCl	0.8333	1.196×10^{-26}	1	2.143	2.035×10^{-26}	1
TFC[1] MT-1	DI water/1 M NaCl	7.083	7.349×10^{-24}	614.1	13.29	4.854×10^{-23}	238.5
TFC[1] MT-2	DI water/1 M NaCl	12.92	4.460×10^{-23}	3727	26.87	4.012×10^{-22}	1971
TFC[1] MT-3	DI water/1 M NaCl	26.67	3.922×10^{-22}	3.278×10^4	54.58	3.363×10^{-21}	1.652×10^4
TFC[1] MT-5	DI water/1 M NaCl	21.67	2.104×10^{-22}	1.759×10^4	49.29	2.477×10^{-21}	1.216×10^4
TFC[2] Control	DI water/1 M NaCl	10.21	2.201×10^{-23}	1	19.89	1.627×10^{-22}	1
TFC[2] MS-10	DI water/1 M NaCl	12.36	3.905×10^{-23}	1.774	23.64	2.732×10^{-22}	1.679
TFC[2] MS-25	DI water/1 M NaCl	16.38	9.089×10^{-23}	4.129	24.09	2.891×10^{-22}	1.777
TFC[2] MS-50	DI water/1 M NaCl	18.61	1.333×10^{-22}	6.056	27.49	4.296×10^{-22}	2.64
TFC[2] MS-75	DI water/1 M NaCl	21.94	2.184×10^{-22}	9.923	29.83	5.489×10^{-22}	3.373
TFC[2] MS-100	DI water/1 M NaCl	16.41	9.139×10^{-23}	4.152	26.93	4.039×10^{-22}	2.482
TFC[3] Control	10 mM NaCl/ 2 M NaCl	16.84	3.517×10^{-23}	1	28.42	1.691×10^{-22}	1
TFC[3] TFN0.5	10 mM NaCl/ 2 M NaCl	30.52	2.094×10^{-22}	5.953	56.85	1.353×10^{-22}	8.004

Table 3 (continued) | Energy parameters affected modifying the support layer of the membranes and operational modes

1B Membrane	2B Feed solution/ Draw solution	3B Pure water flux J_v under FO mode (L/m²-h)	4B $\varphi_F = \frac{E_{1F}}{E_0}$ under FO mode	5B θ_F under FO mode	6B Pure water flux J_v under PRO mode (L/m²-h)	6B $\varphi_P = \frac{E_{1F}}{E_0}$ under PRO mode	7B θ_F under PRO mode
TFC[3] TFN0.75	10 mM NaCl/ 2 M NaCl	40.84	5.017×10^{-22}	14.26	70.25	2.554×10^{-21}	15.10
TFC[3] TFN1	10 mM NaCl/ 2 M NaCl	43.16	5.922×10^{-22}	16.84	77.89	3.481×10^{-21}	20.59

Note: columns A under RO mode, columns B under FO mode. Calculation methods for Table 3 are similar to that in Table 2. The initial total pressure of fluid in columns A is 1 bar, and the initial total pressure (ΔP) of fluid in columns B are produced by the salt concentration differences.

Table 4 | Energy parameters affected by structural parameters

membrane composition	The method of mitigate ICP phenomenon	Structural parameter S^c (μm)	Feed solution/ Draw sloution	φ_F under FO mode	θ_F under FO mode	φ_P under PRO mode	θ_P under PRO mode	Ref
POD – TFC	Control	797	DI water /2 M NaCl	3.102×10^{-23}	1	5.377×10^{-22}	1	[56]
40 mol % PTA – TFC	In-situ mineralization	236	DI water /2 M NaCl	2.482×10^{-22}	8.001	2.260×10^{-21}	4.203	[56]
TFC	Control	4834	DI water /2 M NaCl	3.514×10^{-25}	1	1.320×10^{-24}	1	[57]
TFC32 (15/10/75)wt% PSf /$CaCO_3$/NMP	Chemical-etching	525	DI water /2 M NaCl	1.234×10^{-22}	393.7	6.189×10^{-22}	468.9	[57]
TFC M-0	Control	2223	DI water /2 M NaCl	1.734×10^{-24}	1	1.925×10^{-23}	1	[72]
TFC M-5 5% wt% ZnO to PVDF	Chemical-etching	413	DI water /2 M NaCl	5.054×10^{-23}	29.15	1.135×10^{-22}	5.897	[72]
Unmodified-TFC	Control	2410	DI water /2 M NaCl	2.375×10^{-24}	1	3.394×10^{-22}	1	[73]
Modified-TFC non-swelling hydrophobic fiber	Surface modification	193	DI water /2 M NaCl	3.167×10^{-22}	84.46	1.027×10^{-21}	3.025	[73]
TFC-control	Control	1011	DI water /2 M NaCl	1.188×10^{-22}	1	2.958×10^{-22}	1	[59]
TFC-25.0 (11.25/3.75, wt%) PSf /BPSH100-BPS0	Blending hydrophilic components	397	DI water /2 M NaCl	4.918×10^{-22}	4.139	3.017×10^{-21}	10.10	[59]

Calculation methods for Table 4 are similar in Tables 2, 3. The initial total pressure (ΔP) of fluid is produced by the salt concentration differences.

polytriazole-co-polyoxadiazolecopolymers is optimal for promising porous substrates (Fig. 1A: $y = 0.9147x^{-1.862}$, $R^2 = 0.9752$ under the FO mode; $y = 0.8744x^{-1.179}$, $R^2 = 0.9467$ under the PRO mode); (2) $CaCO_3$ nanoparticles dispersed in PSf matrix were effectively etched with hydrochloric acid to increase the substrate porosity (Fig. 1B: $y = 0.9518\ x^{-2.655}$, $R^2 = 0.9981$ under the FO mode; $y = 1.0558\ x^{-2.717}$, $R^2 = 0.9962$ under PRO mode); (3) the modified polyvinylidene fluoride high porosity and large amounts of surface membrane pores were prepared with zinc oxide nanoparticles (Fig. 1C: $y = 0.9438\ x^{-2.024}$, $R^2 = 0.9948$ under FO mode; $y = 0.8744\ x^{-1.179}$, $R^2 = 0.9238$ under PRO mode); (4) the modified nanofiber exhibited slightly higher structural parameter than the pre-wetted thin composite membrane (Fig. 1D: $y = 1.0016\ x^{-1.747}$, $R^2 = 0.9999$ under FO mode; $y = 0.9976\ x^{-0.455}$, $R^2 = 0.9971$ under PRO mode); and (5) the addition of disulfonated poly (arylene ethersulfone) hydrophilic-hydrophobic multiblock copolymer in the polysufone substrates enhance hydrophilicity and porosity of membrane (Fig. 1E: $y = 0.9348x^{-1.405}$, $R^2 = 0.9072$ under FO mode; $y = 0.9295x^{-2.349}$, $R^2 = 0.9588$ under PRO mode). Therefore, the results show that the model can be unified as $\theta = a(S/S_C)^b$ with a being about 1 and b being negative. The result of reducing ICP by reducing the value of structural parameter S could enhance the membrane energy transfer efficiency, which is consistent with previous studies[59,60]. Table 4 shows that using the two energy parameters can easily compare the results obtained from different studies. Of the five different modification methods, membranes using nano-$CaCO_3$ particles as sacrificial component has the largest θ and with a steepest improvement in the φ value (Table 4), demonstrating that the method may be the best to mitigate ICP phenomenon among the five methods.

Moreover, φ and /or θ can be used to analyze the impact of changing a single factor on the energy transfer efficiency. Figure 2 shows the relationships between the concentration of incorporated nanoparticle and the membranes' energy transfer efficiency coefficients φ. Adding different nanomaterials can lead to different models (improvement) for φ. Through these models, it is possible to digitally analyze how much the additional nanoparticles. Therefore, these equations indicate the relationship between the physical and chemical properties of membrane and the energy transfer efficiency of the membrane, which opens a window to study how to reduce energy consumption by improving the physical and chemical parameters of the membrane.

Implications

Herein, the parameter θ has been evaluated under the three modes. However, it could have a wider range of applications. As long as a method affects the fluid (gas, water, and organic phases, etc.) flow rate out of the membrane, which can be evaluated by θ. Under direct contact membrane distillation (DCMD) mode, as shown in Table 5, parameter θ evaluates the optimal method independent of membrane performance. The conclusion further confirms that it is unscientific to screen the optimal method by membrane performance.

Scientific data alone is often meaningless, and its value needs to be assessed in a system. θ is as an evaluation parameter, which is the link for establishing the comparison of modified methods. The main function of parameter θ as an evaluation parameter is reflected in two aspects: (1) analyze the effect of the modified method on the energy transfer efficiency and its superiority compared with other modified methods; (2) by analyzing the differences of multiple modification strategies, one can identify the future research directions with reasonable theoretical support. The content of the article on how parameters are evaluated for modification methods has been discussed earlier. The following content uses the parameter θ to analyze a series of modified methods for improving the membrane performances, and gives a reasonable scientific research direction. The scientific research should be to choose the

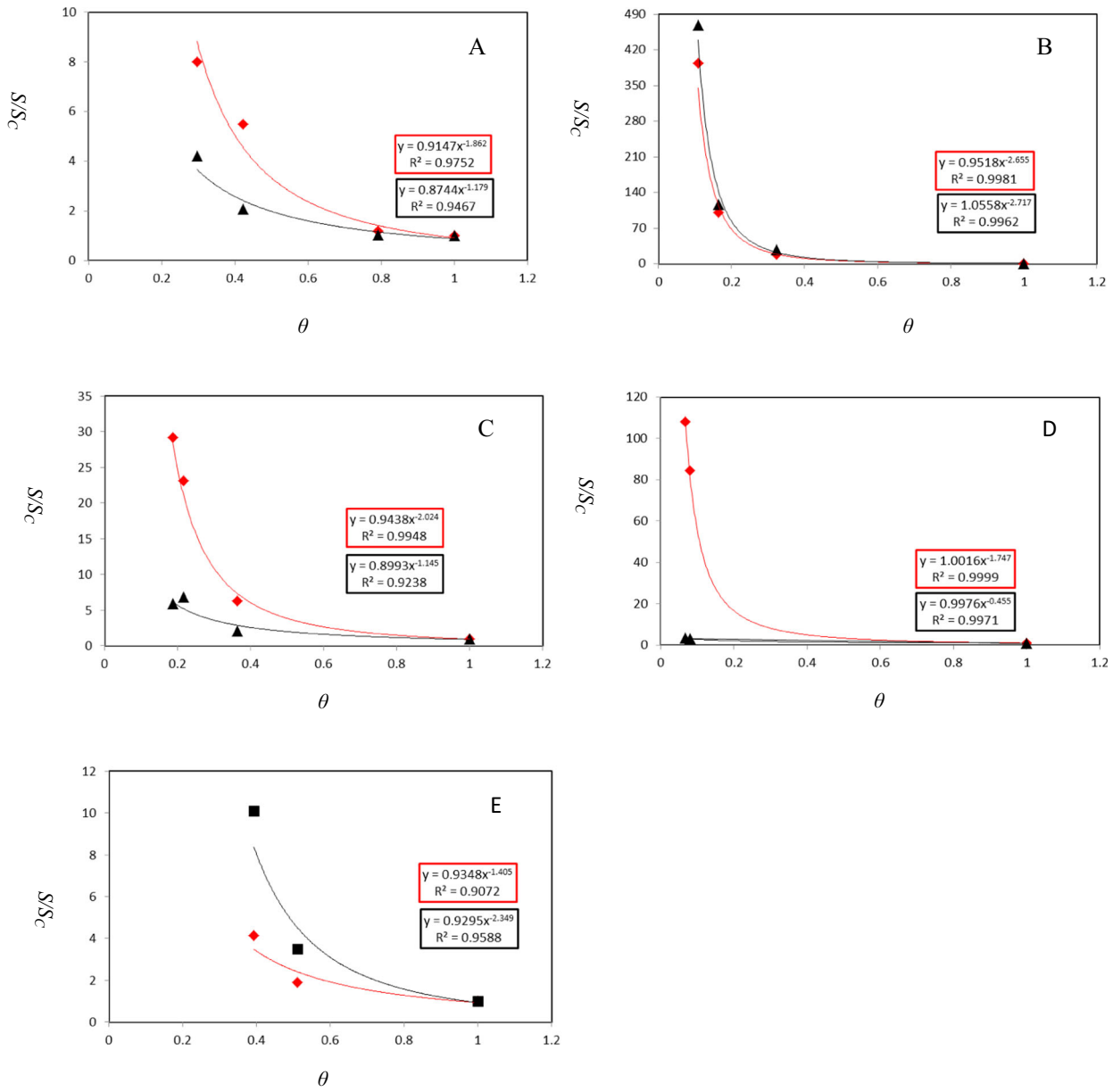

Fig. 1 | The relationship between S/S_c and θ for mitigating ICP phenomenon with different methods under FO mode (◆) or PRO mode (▲). (**A**) In situ mineralization[56]; (**B**) chemical-etching[57]; (**C**) chemical-etching[58]; (**D**) surface modification[72]; and (**E**) blending hydrophilic components[73].

research direction with relatively comparative advantages from the big aspects. Furthermore, the shortcomings of researches are looked for from a small aspect, and the advantages of other researches are learned from to supplement its shortcomings. In the following, the parameter θ was utilized to evaluate the modified methods, and give an optimal research direction.

Under the FO /PRO/RO mode, θ as an evaluation parameter analyzes the completely different laws shown by the data, and its difference represents its irreplaceability and new theoretical direction (Table 6). Surprisingly, the data clearly shows the relatively advantageous of several research directions as follows: (1) the modified support layer could be more conducive to improving the energy conversion efficiency than the modified active layer. For example, the maximum θ values of the modified support layer and the modified active layer is 3.278×10^4 (Table 3) and is 39.68 (Table 2), respectively; (2) modifying the structure of the membrane often gives a much higher θ value (The modified structure $\theta = 39.68$, The modified surface hydrophilicity $\theta = 2.990$), and thus, could be the more efficient way to improve the energy transfer efficiency than the modified properties; and (3) the synergistic effect of multiple strategies is better than a single strategy, but the difference is not significant.

When the research focuses on the point, we need to analyze the deficiencies of different modification methods and find technical routes for improvement. Pore size is an important characteristic of membrane morphology. Herein, the effect of pore size change on parameter θ was analyzed as shown in Table 7. Firstly, it is the most conventional law that the energy transfer efficiency of membranes with larger pore size increases. Secondly, basic materials play a crucial role in energy transfer efficiency, such as graphene oxide as a new type of membrane material. A nanostrand-channelled graphene oxide ultrafiltration membrane with gold nanoparticles has a best performance of energy transfer efficiency at Table 7. But, the use of metal nanoparticles is not an effective method to improve energy transfer efficiency of a membrane. In Table 7, two more effective methods are

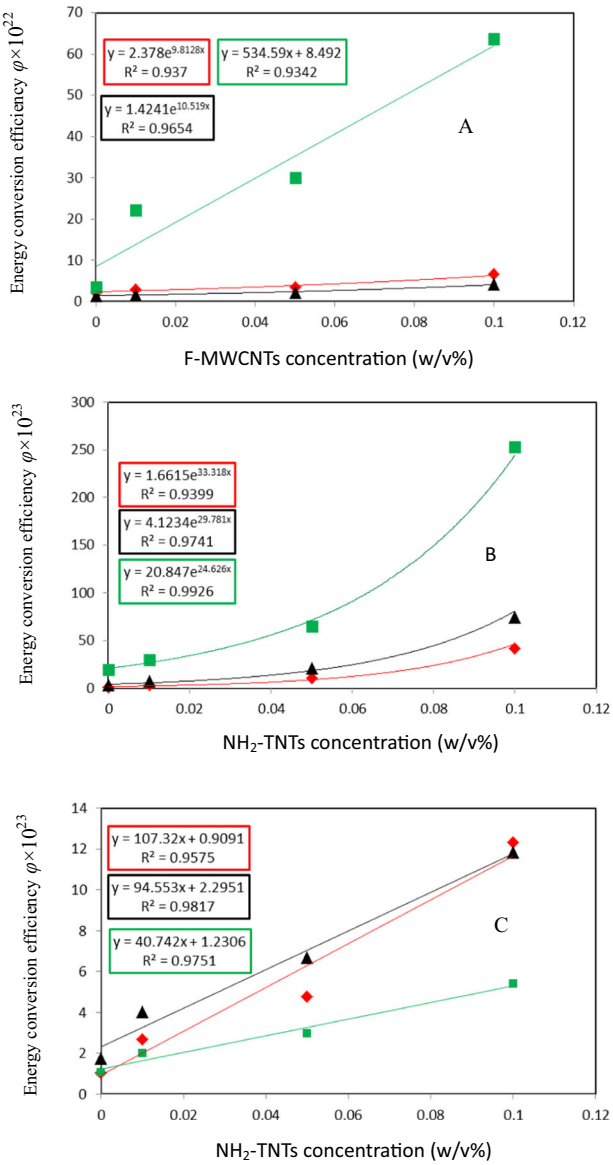

Fig. 2 | Established formulas to reveal the relationship between nanoparticle concentration and the membrane energy transfer efficiency coefficient under RO (◆), FO (▲) or PRO mode (■). A F-MWCNTs[24]; (**B**) NH_2-TNTs[48]; and (**C**) HNTS[69].

provided for us: Method 1 is the supramolecular interaction facilitated block copolymer assembly technology; Method 2 is to enhance the membrane surface porosity and unify membrane pore distribution technology. When designing the modified method obtains an efficient energy transfer of membrane, we can choose to use the above two methods to optimize the membrane pores on the basis that the membrane material is graphene oxide. Here, the provision of this optimization research idea does not indicate a certain feasibility of the operation. Therefore, when there are certain obstacles in the implementation of this route, this parameter θ can be further used to find more optimal research ideas. The more θ values are introduced here, the clearer the relatively scientific direction and the more reasonable research ideas introduced by science can be considered. However, this is a function that the current parameters do not have on the analysis modification method.

Further studies are needed on the effect of different characteristics of the membrane on the energy transfer efficiency. Indeed, the new energy parameters will offer new tools to answer some important questions.

Hence, the study focuses on the key knowledge gaps in membrane science: (1) there is no parameter to construct the relationship between membrane performance and energy consumption; (2) The lack of evaluation system for modification methods leads to relatively isolated research on modification methods. Therefore, φ, as a novel energy parameter, is established to express the membrane performance, which shows that the energy transfer efficiency of membrane is about 10^{-23}. The expression of φ on the membrane performances is similar to other similar parameters, such as A, J_w, k, etc., but it is expressed from an energy perspective. Based on this, a novel system can digitally evaluate the multiple times that each method improves the energy transfer efficiency of the modified membrane compared to the energy transfer efficiency of the pristine membrane. The system θ was used to analyze the modification methods of the membranes, and it was concluded that the most effective modification method can improve the energy transfer efficiency of the modified membrane to 3.278×10^4 times that of the pristine membrane. However, this still indicates that membrane modification methods need further research to find new optimization strategies. This novel evaluation system θ can compare the influence of different modification methods on the energy transfer efficiency of membranes, and provide data guidance for the optimization route of modification methods in the future. This study not only solves the key knowledge holes existing in membrane science, but also has a good guiding value for the application of membrane science.

Reporting summary

Further information on research design is available in the Nature Research Reporting Summary linked to this article.

Table 5 | Parameter θ affected by the modified DCMD performance

Membrane	Preparation method	Feed solution	Temperature (∘C)	*J* water flux (L m^{-2} h^{-1} ba^{r-1})	θ	Ref.
M-O membrane	Blending	35 g/L NaCl	53/20	12.45	1	[74]
M-2 membrane	Blending PVDF/nano-$CaCO_3$	35 g/L NaCl	53/20	14.5	1.580	[74]
M1 membrane	PEG/LiCl mixed additives	35 g/L NaCl	50/20	17.59 ± 0.6	1	[75]
M-5 membrane	PEG/LiCl mixed additives	35 g/L NaCl	50/20	23.57 ± 0.3	2.406	[75]
PVD	Incorporating magnetite NP in PVDF	3.5 wt% NaCl	60/20	11.2	1	[76]
PVD-NP	Incorporating magnetite NP in PVDF	3.5 wt% NaCl	60/20	14.9	2.355	[76]
M3-F4	Fabricated by the immersion-deposition method	3.5 wt% NaCl	50/20	4.29	1	[77]
M3	Fabricated by the immersion-deposition method	3.5 wt% NaCl	50/20	7.86	6.150	[77]
M1 membrane	Tuning the two-stage phase inversion process	35 g/L NaCl	55/25	20	1	[78]
M8 membrane	Tuning the two-stage phase inversion process	35 g/L NaCl	55/25	29	3.049	[78]

Calculation methods for Table 5 are similar in Tables 2, 3.

Table 6 | Influence of modification methods on the energy transfer efficiency ratio

Serial number- Membrane	Modified method	θ_R under RO mode	θ_F under FO mode	θ_P under PRO mode	Ref.
1-TFC	Surface hydrophilicity	2.990	2.974	17.84	24
2-TFC	Surface morphology	39.68	23.76	12.84	44
3-TFC	Surface morphology and hydrophilicity	4.184	3.980	3.279	68
4-TFC	Hydrophilicity and surface morphology	11.80	6.785	5.136	69
5- TFC	Hydrophilicity and membrane morphology of modified support layer	1.969×10^4	3.278×10^4	1.652×10^4	70
6-TFC	Hydrophilicity and membrane morphology of modified support layer	3.095	9.923	3.373	71
7- TFC	Membrane morphology of modified support layer	15.70	16.84	20.59	61
8-TFC	Membrane morphology	~	8.001	4.203	56
9-TFC	Membrane morphology	~	393.7	468.9	57
10-TFC	Membrane morphology	~	29.15	5.897	72
11- TFC	Hydrophilicity and membrane morphology	~	84.46	3.025	73
12-TFC	Hydrophilicity and membrane morphology	~	4.139	10.10	59

Calculation methods for Table 6 are similar in Tables 2, 3.

Table 7 | Parameter θ affected by the modified pore size

Membrane	Modified method	R-Pore diameter (nm)	$S = \frac{R_P}{R_m}$	Water flux (L m^{-2} h^{-1} ba^{r-1})	θ	Ref
NSC-GO membrane-CK	Nanostrand-channelled graphene oxide ultrafiltration membranes with 21,23-H-porphyrin tetratosylate	1.7	1	235 ± 18	1	79
NSC-GO membrane-MO	Nanostrand-channelled graphene oxide ultrafiltration membranes with gold particles	5	2.941	593 ± 31	16.07	79
GO membrane-CK	membrane assembled from g-C_3N_4 nanosheets with Evans Blue molecules	3.1	1.	22	1	80
GO membrane-MO	Membrane assembled from g-C_3N_4 nanosheets with gold nanoparticles	5	1.613	26	1.651	80
M6-S_3/4-24 membrane -CK	Isoporous membranes with supramolecular interaction facilitated block copolymer assembly	7.32	1	7.2	1	81
PS75-b-P4VP25100d membrane -MO	Isoporous membranes with supramolecular interaction facilitated block copolymer assembly	16.13	2.204	320	8.779×10^4	81
PES membrane-CK	polyethersulfone /cellulose nanocrystals nanocomposite membranes	12	1	13.9	1	82
PES membrane-MO-1	PES ultrafiltration membranes by imidazolebased deep eutectic solvents	32.5	2.708	60	80.43	83
PES membrane-MO-2	PES membranes with combining the mixed solvent phase separation in the NMP/nonane mixed solvent system	20	16.67	120.9	658.0	84

Calculation methods for Table 7 are similar in Tables 2, 3.

Data availability

The data generated or analysed during this study are included in this published article. Source data are provided in this paper. Source data are also available on Figshare.

Received: 14 August 2023; Accepted: 19 February 2024;
Published online: 11 March 2024

References

1. Logan, B. E. & Elimelech, M. Membrane-based processes for sustainable power generation using water. *Nature* **488**, 313–319 (2012).
2. Liu, S., Qian, Y., Li, D., Klemeš, J. & Yang, S. Multi-Scenario scheduling optimisation for a novel Double-Stage ammonia absorption refrigeration system incorporating an organic Rankine cycle. *Energ. Convers. Manag.* **270**, 116170 (2022).
3. Gu, B. X., Wu, H. H., Sun, D., Ji, Y. L. & Gao, C. J. Zwitterionic cyclodextrin membrane with uniform subnanometre pores for high-efficient heavy metal ions removal. *J. Membr. Sci.* **688**, 22123 (2023).
4. Liang, Y., Dudchenko, A. V. & Mauter, M. S. Novel method for accurately estimating membrane transport properties and mass transfer coefficients in reverse osmosis. *J. Membr. Sci.* **679**, 121686 (2023).
5. Lyly, L. H. T., Chang, Y.-S., Ng, W.-M., Lim, J.-K. & Derek, C.-J.-C. et al. Development of membrane distillation by dosing SiO_2-PNIPAM with thermal cleaning properties via surface energy actuation. *J. Membr. Sci.* **19**, 119193 (2021).
6. Siddiqui, M. U., Generous, M. M., Qasem, N. A. A. & Zubair, S. M. Explicit prediction models for brackish water electrodialysis desalination plants: Energy consumption and membrane area. *Energ. Convers. Manag.* **261**, 115656 (2022).

7. Sigurdardottir, S. B., DuChanois, R. M., Epsztein, R., Pinelo, M. & Elimelech, M. Energy barriers to anion transport in polyelectrolyte multilayer nanofiltration membranes: Role of intra-pore diffusion. *J. Membr. Sci.* **603**, 117921 (2020).
8. Gao, T., Zhang, H., Xu, X., Teng, J. & Lu, M. Enhanced water and energy recovery from anaerobic osmotic membrane bioreactors treating waste activated sludge based on the draw solution concentration and temperature regulation. *Chem. Eng. J.* **417**, 129325 (2021).
9. Khaled, T., Haamid, S. U., Catherine, N. M. & Md, S. R. Energetic and economic feasibility of a combined membrane-based process for sustainable water and energy systems. *Appl. Energ.* **264**, 114699 (2020).
10. Nguyen, T. T., Adha, R. S., Field, R. W. & Kim, I. S. Extended performance study of forward osmosis during wastewater reclamation: Quantification of fouling-based concentration polarization effects on the flux decline. *J. Membr. Sci.* **618**, 118755 (2021).
11. Zhou, L., Yu, H., Hossain, M. Y., Chen, F. & Du, C. et al. Fabrication of high-performance forward osmosis membrane based on asymmetric integrated nanofiber porous support induced by a new controlled photothermal induction method. *Chem. Eng. J.* **470**, 144366 (2023).
12. Zhou, Y., Shi, Y., Cai, D., Yan, W., Zhou, Y. & Gao, C. Support-free interfacial polymerized polyamide membrane on a macroporous substrate to reduce internal concentration polarization and increase water flux in forward osmosis. *J. Membr. Sci.* **689**, 122165 (2024).
13. Wu, X., Fang, F., Zhang, B., Wu, J. J. & Zhang, K. Biogenic silver nanoparticles-modified forward osmosis membranes with mitigated internal concentration polarization and enhanced antibacterial properties. *NPJ Clean. Water* **5**, 41 (2022).
14. Joshi, U. S., Anuradha & Jewrajka, S. K. Tight ultrafiltration and loose nanofiltration membranes by concentration polarization-driven fast layer-by-layer self-assembly for fractionation of dye/salt. *J. Membr. Sci.* **669**, 121286 (2023).
15. Arjmandi, A., Peyravi, M., Arjmandi, M. & Altaee, A. Exploring the use of cheap natural raw materials to reduce the internal concentration polarization in thin-film composite forward osmosis membranes. *Chem. Eng. J.* **398**, 125483 (2020).
16. Zhang, X., Xiong, S., Liu, C.-X., Shen, L. & Ding, C. et al. Confining migration of amine monomer during interfacial polymerization for constructing thin-film composite forward osmosis membrane with low fouling propensity. *Chem. Eng. Sc.* **207**, 54–68 (2019).
17. Xiong, S., Xu, S., Zhang, S., Phommachanh, A. & Wang, Y. Highly permeable and antifouling TFC FO membrane prepared with CD-EDA monomer for protein enrichment. *J. Membr. Sci.* **572**, 281–290 (2019).
18. Xie, Q. L., Zhang, S. S., Hong, Z., Zeng, H. M. B. & Gong, X. et al. A novel double-modified strategy to enhance the performance of thin-film nanocomposite nanofiltration membranes: Incorporating functionalized graphenes into supporting and selective layers. *Chem. Eng. J.* **368**, 186–201 (2019).
19. Zuo, H. R., Shi, P. & Duan, M. A review on thermally stable membranes for water treatment: Material, fabrication, and application. *Sep. Purif. Technol.* **236**, 116223 (2020).
20. Saleh, H., Shakeri, A. & Lammertink, R. G. H. Thermo-responsive graft copolymer PSf-g-PNIPM: Reducing the structure parameter via morphology control of forward osmosis membrane substrates. *J. Membr. Sci.* **661**, 120794 481 (2022).
21. Han, C., Zhang, X., Ding, C., Xiong, S. & Yu, X. et al. Improved performance of thin-film composite membrane supported by aligned nanofibers substrate with slit-shape pores for forward osmosis. *J. Membr. Sci.* **612**, 118447 (2020).
22. Venault, A., Chang, K.-Y. & Maggay, I. V. Assessment of the DCMD performances of poly(vinylidene difluoride) vapor-induced phase separation membranes with adjusted wettability via formation process parameter manipulation. *Desalination* **560**, 116682 (2023).
23. Liu, C., Lee, J., Small, C., Ma, J. & Elimelech, M. Comparison of organic fouling resistance of thin-film composite membranes modified by hydrophilic silica nanoparticles and zwitterionic polymer brushes. *J. Membr. Sci.* **544**, 135–142 (2017).
24. Amini, M., Jahanshahi, M. & Rahimpour, A. Synthesis of novel thin film nanocomposite (TFN) forward osmosis membranes using functionalized multi-walled carbon nanotubes. *J. Membr. Sci.* **435**, 233–241 (2013).
25. Holland, F., Bragg, R. Fluid flow for chemical engineers. Elsevier Science & Technology. **2** (1995).
26. Blankert, B., Martinez, F. D., Vrouwenvelder, J. S. & Picioreanu, C. Solution-diffusion-electromigration approximation model (SDE-A) for strongly charged, weakly charged and effectively uncharged reverse osmosis membranes. *J. Membr. Sci.* **679**, 121675 (2023).
27. Foo, Z. H., Rehman, D., Coombs, O. Z., Deshmukh, A. & Lienhard V, J. H. Multicomponent Fickian solution-diffusion model for osmotic transport through membranes. *J. Membr. Sci.* **640**, 119819 (2021).
28. Sukitpaneenit, P., Chung, T. S. & Jiang, L. Y. Modified pore-flow model for pervaporation mass transport in PVDF hollow fiber membranes for ethanol–water separation. *J. Membr. Sci.* **362**, 393–406 (2010).
29. Song, S., Rong, L., Dong, K., Liu, X., Le-Clech, P. & Shen, Y. Pore-scale numerical study of intrinsic permeability for fluid flow through asymmetric ceramic microfiltration membranes. *J. Membr. Sci.* **642**, 119920 (2022).
30. Huang, W., Zhao, L., Zhang, J., Wen, H. & Zhu, Z. et al. Template-etched sodium alginate hydrogel as the sublayer to improve the FO performance with double barriers for high metal ion rejection. *Chem. Eng. J.* **413**, 127425 (2021).
31. He, Y., Lin, X., Chen, J.-H. & Zhan, H.-B. Fabricating novel high-performance thin-film composite forward osmosis membrane with designed sulfonated covalent organic frameworks as interlayer. *J. Membr. Sci.* **635**, 119476 (2021).
32. Luo, F., Wang, J., Yao, Z.-K., Zhang, L. & Chen, H.-L. Polydopamine nanoparticles modified nanofiber supported thin film composite membrane with enhanced adhesion strength for forward osmosis. *J. Membr. Sci.* **618**, 118673 (2021).
33. Rui, L., Sylvie, B., Johan, L. N. D. C., Shazad, H. & Ulla, E.-B. et al. Laboratory and pilot evaluation of aquaporin-based forward osmosis membranes for rejection of micropollutants. *Water Res.* **194**, 116924 (2021).
34. Ghorbani, F., Shakeri, A., Vafaei, M. A. & Salehi, H. Polyoxometalate-cored supramolecular star polymers as a novel crosslinker for graphene oxide-based forward osmosis membranes: Anti-fouling, super hydrophilic and high water permeable. *Sep. Purif. Technol.* **267**, 118578 (2021).
35. Daeeun, K., Woobin, B. & Jeonghwan, K. Hybrid forward osmosis/membrane distillation integrated with anaerobic fluidized bed bioreactor for advanced wastewater treatment. *J. Hazard. Mater.* **404**, 124160 (2021).
36. Rong, K. & Zhang, T. C. Forward osmosis: mass transmission coefficient-based models for evaluation of concentration polarization under different conditions. *J. Environ. Eng.* **144**, 04017095 (2017).
37. Rong, K., Zhang, T. C. & Li, T. Forward osmosis: Definition and evaluation of water transmission coefficient. *J. Water Process. Eng.* **20**, 106–112 (2017).
38. Zhang, X., Xiong, S., Liu, C.-X., Shen, L. & Wang, S.-L. et al. Smart TFC membrane for simulated textile wastewater concentration at elevated temperature enabled by thermal-responsive microgels. *Desalination* **500**, 114870 (2021).
39. Sung, J.-I., Luca, F. & Am, J. Real-time fouling monitoring and membrane autopsy analysis in forward osmosis for wastewater reuse. *Water Res.* **197**, 117098 (2021).
40. Wang, P., Cui, Y., Ge, Q.-C., Tew, T.-F. & Chung, T.-S. Evaluation of hydroacid complex in the forward osmosis–membrane distillation (FO–MD) system for desalination. *J. Membr. Sci.* **494**, 1–7 (2015).

41. Xiao, D.-Z., Tang, C.-Y., Zhang, J.-S., Lay, W. C. L. & Wang, R. et al. Modeling salt accumulation in osmotic membrane bioreactors: Implications for FO membrane selection and system operation. *J. Membr. Sci.* **366**, 314–324 (2011).
42. Zhao, L.-H., Wu, C.-R., Lu, X.-L., Ng, D. & Truong, Y. B. et al. Activated carbon enhanced hydrophobic/hydrophilic dual-layer nanofiber composite membranes for high-performance direct contact membrane distillation. *Desalination* **446**, 59–69 (2018).
43. Akther, N., Lin, Y.-Q., Wang, S.-Y., Phuntsho, S. & Fu, Q. et al. In situ ultrathin silica layer formation on polyamide thin-film composite membrane surface for enhanced forward osmosis performances. *J. Membr. Sci.* **620**, 118876 (2021).
44. Ji, D.-W., Xiao, C.-F., Chen, K.-K., Zhou, F. & Gao, Y.-F. et al. Solvent-free green fabrication of PVDF hollow fiber MF membranes with controlled pore structure via melt-spinning and stretching. *J. Membr. Sci.* **621**, 118953 (2021).
45. D'Haese, A. & Yaroshchuk, A. Interplay between membrane imperfections and external concentration polarization. *J. Membr. Sci.* **676**, 121579 (2023).
46. Johnson, D. & Hilal, N. Polymer membranes – Fractal characteristics and determination of roughness scaling exponents. *J. Membr. Sci.* **570–571**, 9–22 (2019).
47. Kim, S. J., Kook, S., O'Rourke, B.-E., Lee, J. & Hwang, M. Y. et al. Characterization of pore size distribution (PSD) in cellulose triacetate (CTA) and polyamide (PA) thin active layers by positron annihilation lifetime spectroscopy (PALS) and fractional rejection (FR) method. *J. Membr. Sci.* **527**, 143–151 (2017).
48. Emadzadeh, D., Lau, W. J., Rahbari-Sisakht, M., Ilbeygi, H., Rana, D., Matsuura, T. & Ismail, A.-F. Synthesis, modification and optimization of titanate nanotubespolyamide thin film nanocomposite (TFN) membrane for forward osmosis (FO) application. *Chem. Eng. J.* **281**, 243–251 (2015).
49. Dutta, S., Gupta, R. S., Manna, K., Islam, S. S. & Bose, S. 'Green-tea' extract soldered triple interpenetrating polymer network membranes for water remediation. *Chem. Eng. J.* **472**, 145008 (2023).
50. Zou, D., Kim, H. W., Jeon, S. M. & Lee, Y. M. Robust PVDF/PSF hollow-fiber membranes modified with inorganic TiO_2 particles for enhanced oil-water separation. *J. Membr. Sci.* **652**, 120470 (2022).
51. Ostadi, M., Kamelian, F. S. & Mohammadi, T. Superhydrophilic micro/nano hierarchical functionalized-CuO/PVDF nanocomposite membranes with ultra-low fouling/biofouling performance for acetate wastewater treatment: MBR application. *J. Membr. Sci.* **676**, 121591 (2023).
52. Zhao, Y.-L., Lai, G.-S., Wang, Y., Li, C. & Wang, R. Impact of pilot-scale PSF substrate surface and pore structural properties on tailoring seawater reverse osmosis membrane performance. *J. Membr. Sci.* **633**, 119395 (2021).
53. Salehi, H.-S., Shakeri, A. & Rastgar, M. Carboxylic polyethersulfone: A novel pH-responsive modifier in support layer of forward osmosis membrane. *J. Membr. Sci.* **548**, 641–653 (2018).
54. Wei, Y., Wang, Y., Wang, L., Yang, H. & Jin, H. et al. Simultaneous phase-inversion and crosslinking in organic coagulation bath to prepare organic solvent forward osmosis membranes. *J. Membr. Sci.* **620**, 118829 (2021).
55. Lin, X., He, Y., Zhang, Y., Yu, W. & Lian, T. Sulfonated covalent organic frameworks (COFs) incorporated cellulose triacetate/cellulose acetate (CTA/CA)-based mixed matrix membranes for forward osmosis. *J. Membr. Sci.* **638**, 119725 (2021).
56. Duong, P. H. H., Chisca, S., Hong, P. Y., Cheng, H. & Nunes, S. P. et al. Hydroxyl Functionalized Polytriazole-co-polyoxadiazole as Substrates for Forward Osmosis Membranes. *Acs. Appl. Mater. Interfaces* **7**, 3960–3973 (2015).
57. Kuang, W., Liu, Z.-N., Yu, H.-J., Kang, G.-D., Jie, X.-M., Jin, Y. & Cao, Y.-M. Investigation of internal concentration polarization reduction in forward osmosis membrane using nano-$CaCO_3$ particles as sacrificial component. *J. Membr. Sci.* **497**, 485–493 (2016).
58. Loeb, S., Titelman, L., Korngold, E. & Freiman, J. Effect of porous support fabric on osmosis through a Loeb–Sourirajan type asymmetric membrane. *J. Membr. Sci.* **129**, 243–249 (1997).
59. Zhang, X. Y., Tian, J. Y., Ren, Z. J., Shi, W. X. & Zhang, Z. B. et al. High performance thin-film composite (TFC) forward osmosis (FO) membrane fabricated on novel hydrophilic disulfonated poly (arylene ether sulfone) multiblock copolymer/polysulfone substrate. *J. Membr. Sci.* **520**, 529–539 (2016).
60. Wen, H., Xu, N., Soyekwo, F., Dou, P. & Liu, C. Towards enhanced performance of fertilizer-drawn forward osmosis process coupled with sludge thickening using a thin-film nanocomposite membrane interlayered with Mxene scaffolded alginate hydrogel. *J. Membr. Sci.* **685**, 121899 (2023).
61. Emadzadeh, D., Lau, W. J., Matsuura, T., Rahbari-Sisakht, M. & Ismail, A.-F. A novel thin film composite forward osmosis membrane prepared from PSf –TiO_2 nanocomposite substrate for water desalination. *Chem. Eng. J.* **237**, 70–80 (2014).
62. Wei, J., Qiu, C.-Q., Tang, C., Wang, R. & Fane, A. G. Synthesis and characterization of flat-sheet thin film composite forward osmosis membranes. *J. Membr. Sci.* **372**, 292–302 (2011).
63. Liang, S., Wu, J., Wang, C., Zhao, X. & Wang, C. et al. Ultra-high selectivity self-supporting symmetric membrane for forward osmosis separation. *Desalination* **534**, 115796 (2022).
64. Duong, P. H. H., Chung, T.-S., Wei, S. & Irish, L. Highly Permeable Double-Skinned Forward Osmosis Membranes for Anti-Fouling in the Emulsified Oil−Water Separation Process. *Environ. Sci. Technol.* **8**, 4537–4545 (2014).
65. Lim, S., Tran, V. H., Akther, N., Phuntsho, S. & Shon, H.-K. Defect-free outer-selective hollow fiber thin-film composite membranes for forward osmosis applications. *J. Membr. Sci.* **586**, 281–291 (2019).
66. Behboudi, A., Ghiasi, S., Mohammadi, T. & Ulbricht, M. Preparation and characterization of asymmetric hollow fiber polyvinyl chloride (PVC) membrane for forward osmosis application. *Sep. Purif. Technol.* **270**, 118801 (2021).
67. Setiawan, L., Wang, R., Li, K. & Fane, A. G. Fabrication of novel poly(amide–imide) forward osmosis hollow fiber membranes with a positively charged nanofiltration-like selective layer. *J. Membr. Sci.* **369**, 196–205 (2011).
68. Chiao, Y. H., Sengupta, A., Chen, S.-T., Huang, S.-H. & Hu, C.-C. et al. Zwitterion augmented polyamide membrane for improved forward osmosis performance with significant antifouling characteristics. *Sep. Purif. Technol.* **212**, 316–325 (2019).
69. Ghanbari, M., Emadzadeh, D., Lau, W. J., Lai, S. O. & Matsuura, T. et al. Synthesis and characterization of novel thin film nanocomposite (TFN) membranes embedded with halloysite nanotubes (HNTs) for water desalination. *Desalination* **358**, 33–41 (2015).
70. Zhang, X., Shen, L., Lang, W.-Z. & Wang, Y. Improved performance of thin-film composite membrane with PVDF/PFSA substrate for forward osmosis process. *J. Membr. Sci.* **535**, 188–199 (2017).
71. Zhang, X., Shen, L., Guan, C.-Y., Liu, C.-X. & Lang, W.-Z. et al. Construction of SiO_2@MWNTs incorporated PVDF substrate for reducing internal concentration polarization in forward osmosis. *J. Membr. Sci.* **564**, 328–341 (2018).
72. Zhao, X.-Z., Li, J. & Liu, C.-K. Improving the separation performance of the forward osmosis membrane based on the etched microstructure of the supporting layer. *Desalination* **408**, 102–109 (2017).
73. Huang, L. W., Arena, J. T. & McCutcheon, J. R. Surface modified PVDF nanofiber supported thin film composite membranes for forward osmosis. *J. Membr. Sci.* **499**, 352–360 (2016).
74. Hou, D., Dai, G., Fan, H., Wang, J. & Zhao, C. et al. Effects of calcium carbonate nano-particles on the properties of PVDF/nonwoven fabric flat-sheet composite membranes for direct contact membrane distillation. *Desalination* **347**, 25–33 (2014).

75. Zheng, L., Wu, Z., Wei, Y., Zhang, Y. & Yuan, Y. et al. Preparation of PVDF-CTFE hydrophobic membranes for MD application: effect of LiCl-based mixed additives. *J. Membr. Sci.* **506**, 71–85 (2016).
76. Agbaje, T. A., Al-Gharabli, S., Mavukkandy, M. O., Kujawa, J. & Arafat, H. A. PVDF/ magnetite blend membranes for enhanced flux and salt rejection in membrane distillation. *Desalination* **436**, 69–80 (2018).
77. Zhang, W., Li, Y., Liu, J., Li, B. & Wang, S. Fabrication of hierarchical poly (vinylidene fluoride) micro/nano-composite membrane with anti-fouling property for membrane distillation. *J. Membr. Sci.* **535**, 258–267 (2017).
78. Zheng, L., Wang, J., Wu, Z., Li, J. & Zhang, Y. et al. Preparation of interconnected biomimetic poly(vinylidene fluoride-co-chlorotrifluoroethylene) hydrophobic membrane by tuning the two-stage phase inversion process. *Acs. Appl. Mater. Interfaces* **8**, 32604–32615 (2016).
79. Huang, H., Song, Z., Wei, N., Shi, L., Mao, Y. & Ying, Y. et al. Ultrafast viscous water flow through nanostrand-channelled graphene oxide membranes. *Nat. Commun.* **4**, 2379 (2013).
80. Wang, Y., Li, L., Wei, Y., Xue, J. & Chen, H. et al. Water transport with ultralow friction through partially exfoliated g-C_3N_4 nanosheet membranes with self-supporting spacers. *Angew. Chem. Int. Ed.* **56**, 8974–8980 (2017).
81. Zhu, G. D., Ying, Y. R., Li, X., Liu, Y. & Yang, C. Y. et al. Isoporous membranes with sub-10 nm pores prepared from supramolecular interaction facilitated block copolymer assembly and application for protein separation. *J. Membr. Sci.* **566**, 25–34 (2018).
82. Zhang, D., Karkooti, A., Liu, L., Sadrzadeh, M. & Thundat, T. et al. Fabrication of antifouling and antibacterial polyethersulfone (PES)/ cellulose nanocrystals (CNC) nanocomposite membranes. *J. Membr. Sci.* **549**, 350–356 (2018).
83. Jiang, B., Zhang, N., Zhang, L., Sun, Y. & Huang, Z. et al. Enhanced separation performance of PES ultrafiltration membranes by imidazolebased deep eutectic solvents as novel functional additives. *J. Membr. Sci.* **564**, 247–258 (2018).
84. Li, P. P., Thankamony, R. L., Li, X., Li, Z. & Liu, X. et al. Nanoporous polyethersulfone membranes prepared by mixed solvent phase separation method for protein separation. *J. Membr. Sci.* **635**, 119507 (2021).

Author contributions

T.L.: Conceptualization, Data curation, Formal analysis, Methodology, Visualization, Writing—original draft, Writing—review & editing. H.Z.: Writing—review & editing. W.D.: Writing—review & editing. J.W.: Writing—review & editing. T.C.Z.: Conceptualization, Writing—review & editing.

Competing interests

The authors declare no competing interests.

Additional information

Supplementary information The online version contains supplementary material available at https://doi.org/10.1038/s41545-024-00310-z.

Correspondence and requests for materials should be addressed to Tian Li, Jinjun Wang or Tiancheng Zhang.